LA-UR-81-896

CONF-810429--3

TITLE: LASERS AS A TOOL FOR PLASMA DIAGNOSTICS

MASTER

AUTHOR(S): Franz C. Jahoda

SUBMITTED TO: Los Alamos Conference on Optics '81

University of California

LOS ALAMOS SCIENTIFIC LABORATORY
Post Office Box 1663 Los Alamos, New Mexico 87545
An Affirmative Action/Equal Opportunity Employer

Form No. 836 R3
St. No. 2629
12/78

UNITED STATES
DEPARTMENT OF ENERGY
CONTRACT W 7405-ENG 36

LASERS AS A TOOL FOR PLASMA DIAGNOSTICS

Franz C. Jahoda

Lecture Notes for Mini-Course
Los Alamos Conference on Optics '81
April 6, 1981

ABSTRACT

Lasers can be used as non-perturbative probes to measure many plasma parameters.

Plasma refractivity is primarily a function of electron density, and interferometric measurements of phase changes with either pulsed or CW lasers can determine this parameter with spatial or temporal resolution over several orders of magnitude sensitivity by using laser wavelengths from the near UV to the far infrared. Sub-categories include density gradient and/or turbulence determinations from the laser beam deflection and magnetic field magnitudes from polarization rotation by bi-refringence.

Laser scattering from free electrons yields the most fundamental electron temperature measurements in the plasma parameter range where individual scattering events are uncorrelated in phase and ion temperature or plasma wave and turbulence structure in the opposite limit. The smallness of the scattering cross-section generally limits these experiments to single points in space and time using powerful Q-switched lasers. Extensions in both spatial and temporal domains are current research topics.

Laser scattering from bound electrons can be many orders of magnitude larger if the laser is matched to appropriate resonance frequencies and can be used in specialized circumstances for measuring low-ionized impurity or dominant species neutral concentrations and velocities.

The mini-course will emphasize the fundamental physics underlying the many techniques and draw on particular applications examples based largely on the author's experience in magnetic confinement fusion research.

---

1. INTRODUCTION

We limit ourselves in this mini-course to laser frequencies much larger than any characteristic plasma frequency. In this limit the interaction between the EM wave and plasma is weak and manifests itself primarily by small changes in the refractive index (ratio of phase velocity in vacuum to that in

the plasma) and some scattering. This is desirable for a diagnostic measurement of ambient plasma parameters without perturbation by the measurement itself.

Furthermore the laser wavelengths are always small compared to the scale lengths for macroscopic plasma parameter changes. All derivations therefore assume plane waves traversing infinite homogeneous media. These simplifications do not affect the sample experiments to be presented, but should not be forgotten before making extrapolations to extreme situations.

There are a few general considerations pertinent to the usefulness of any diagnostic technique. Most obvious, of course, is whether the sensitivity range covers the anticipated range of values of the parameter to be measured. Adequate calibration may or may not present problems. Hardly less basic is the attainable signal-to-noise ratio and signal-to-background ratio. The distinction implied here is that the former refers to measurement accuracy of the method under more or less idealized circumstances, whereas the latter may be less due to competing effects, such as plasma self-luminosity. Of great practical significance is the cost and complexity of actual execution. This includes geometrical accesibility, available ports and permissable window materials, often substantial requirements on eliminating electromagnetic interference, and increasingly, automation of data acquisition. Although the bulk of the work usually resides in these mundane matters, they are usually both so specific to the particular circumstances and best learned by practical experience, that relatively little will be said about them in the course. None-the-less, this matter of practical adaptability should be the dominant criterion against which everything else is judged.

One theme that will run through everything to be presented is space and time resolution and space and time coverage. By resolution is meant how precisely in space and time a measurement can be localized as opposed to some average value over an extended spatial or temporal range. By coverage, for lack of a better word, is meant how many simultaneous localized space measurements and how many consecutive localized time measurements can be made. This is significant because generally the plasma to be studied is assumed to be of a pulsed nature with both limitations on rep rate and detailed

reproducibility, making shot-by-shot scans of spatial and temporal behavior less valuable than fuller coverage on each individual discharge.

Considered as classical electromagnetic phenomena, refraction and scattering are separate manifestations of the re-radiation of incident light by free or bound electrons. The former is the coherent superposition of the re-radiation in the forward direction added to the incident radiation, and the latter is a coherent or incoherent summation of the re-radiation in other directions.

It is a remarkable fact--stated in other words, a manifestation of the fantastic power of Maxwell's equations--that this basically complicated problem of a self-consistent solution for electric fields acting on charges, which then themselves become sources of fields interacting with all other charges, can be characterized for any particular medium by one complex number (possibly one complex tensor if there are preferred spatial directions in the medium) inserted into the wave propagation equation.

(Sometimes the basic simplicity tends to get lost among 1) the variety of related ways the basic datum can be expressed--e.g. refractive index, dielectric constant, susceptibility, 2) a doubling of names and a second complex value if magnetization is important in the medium, and 3) a bewildering variety of units, normalizations and symbols chosen by different authors. For an excellent reference on the basics and an underlying physical intuition see Chapters 28-34, The Feynman Lectures on Physics, Vol. I, Addision-Wesley (1963)).

II. REFRACTIVITY

(Basic reference[1] referred to hereafter as I.)

A. Theory

The refractive index, μ, is defined as kc/ω where $k = k(\omega)$ is the transverse ($\vec{k}\cdot\vec{E}=0$) plane wave solution to the wave equation (11.2.8 in I.) derived from Maxwell's equations. It is solved for a medium of free electrons in I. for 3 cases:

1) no collisions, no external field

$$\mu = \left[1 - \frac{\omega_p^2}{\omega^2}\right]^{1/2} \qquad (11.1.16)$$

2) no collisions, applied field along $\vec{k}$

$$\mu_\pm = \left[1 - \frac{\omega_p^2}{\omega^2(1 \pm \omega_e/\omega)}\right]^{1/2} \qquad (11.2.26)$$

3) with collisions, no external field

$$\mu = \left[1 - \frac{\omega_p^2}{\omega^2(1 + i\nu/\omega)}\right]^{1/2} \qquad (\text{from } 11.2.19)$$

In these equation

$\omega = 2\pi c/\lambda$ is the radian frequency of the propagating laser wave

$\omega_p = (4\pi ne^2/m)^{1/2}$ is the plasma frequency

$\omega_e = eB_o/mc$ is the cyclotron frequency

ν is the electron-ion 90^o collision frequency.

The system of units throughout is c.g.s.

General remarks:

1) The non-magnetized, non-collisional result for free electron changes to

$$\mu = \left[1 + \frac{\omega_p^2}{\omega_c^2 - \omega^2}\right]^{1/2}$$

when the equation of motion of a bound electron is written as a harmonic oscillator with "spring" constant, $m\omega_o^2$. This can be of quite different magnitude (in the case of near resonance, $\omega \approx \omega_o$, a damping term must be included in the equation of motion to keep everything finite). We make the justifiable assumption in I. that ω_o in the case of incomplete ionization of the major species or impurities is always $>> \omega$, and, therefore, the free electron refractivity is the dominant contribution.

2) The double sign in the magnetic field case indicates bi-refringence and the choice of coordinates, or basis-vectors, that the fundamental modes (i.e., the ones propagated without change of polarization state) are circular. In consequence a linear polarization rotates as it propagates (Faraday Rotation - 11.3.18 in I.). If perpendicular magnetic fields are also included in the equations of motion, a linear bi-refringence emerges. The multiplier term on ω_p^2/ω^2 in this case is itself proportional to $(\omega_e/\omega)^2$ instead of (ω_e/ω), and in the limit $\omega_e << \omega$, transverse fields are less significant.

3) The appearance of an imaginary part to the refractive index (or, equivalently, the k vector) in the case of collisions indicates the wave is attenuated as it propagates. Strong enough absorption would eventually violate our requirement that the laser beam itself not change the plasma parameters. The collision frequency varies as $n/T^{3/2}$, so that classical absorption (inverse bremsstrahlung) is most important at high density and low temperature. A typical calculation indicates that for a 5 eV, $n = 10^{17} cm^{-3}$ plasma, a 1 MW laser of 100 ns pulse duration focused into 1 mm^2 leads to e-

energy increase by absorption of ~25% of the thermal energy originally present. We do not consider absorption further in these notes.

4) Since the refractive index--i.e., phase velocity--is proportional to electron density it immediately follows from geometrical otics that laser light will be deviated from straight line propagation if it encounters transverse density gradients. A derivation of the angular deflection leads to Eq. (11.3.13a) in I. This effect itself can be a useful diagnostic (Schlieren, shadowgraphy) for density gradients and fluctuations but it also places limitations on "straight-through" measurements like interferometry and Faraday rotation. Note, in particular, since both the refractive index and the angular deviation scale as wavelength squared, but in every kind of interferometry the unit of measurement (fringe displacement) is the wavelength itself, the bending effects get relatively worse as sensitivity is increased by going to longer wavelength. Even if imaging of the region of interest is used, whereby a lens compensates the zero-order path difference for deflected rays, the derivation culminating in 11.3.9 in I. indicates a remaining relative fringe error that scales with λ^2.

A summary of this section is provided by Fig. 1. Starting with a given laser wavelength on the abscissa, the fringe shift for a given $\int n_e d\ell$, the Faraday rotation per 1.7 kG for a given $\int n_e d\ell$ (linearly scalable to the desired field value) and the angular deviation for a given $\int \frac{dn_e}{dr} d\ell$ can be obtained by vertical interpolation (logarithmic scale !) between fixed values of these parameters. The critical density at which the laser frequency equals the plasma frequency is also plotted. Longer wavelengths will not propagate at all, and the discussion of the various diagnostics generally assumes a wavelength at least an order of magnitude below the cut-off. Conversions to several frequently used units that replace wavelength are also indicated.

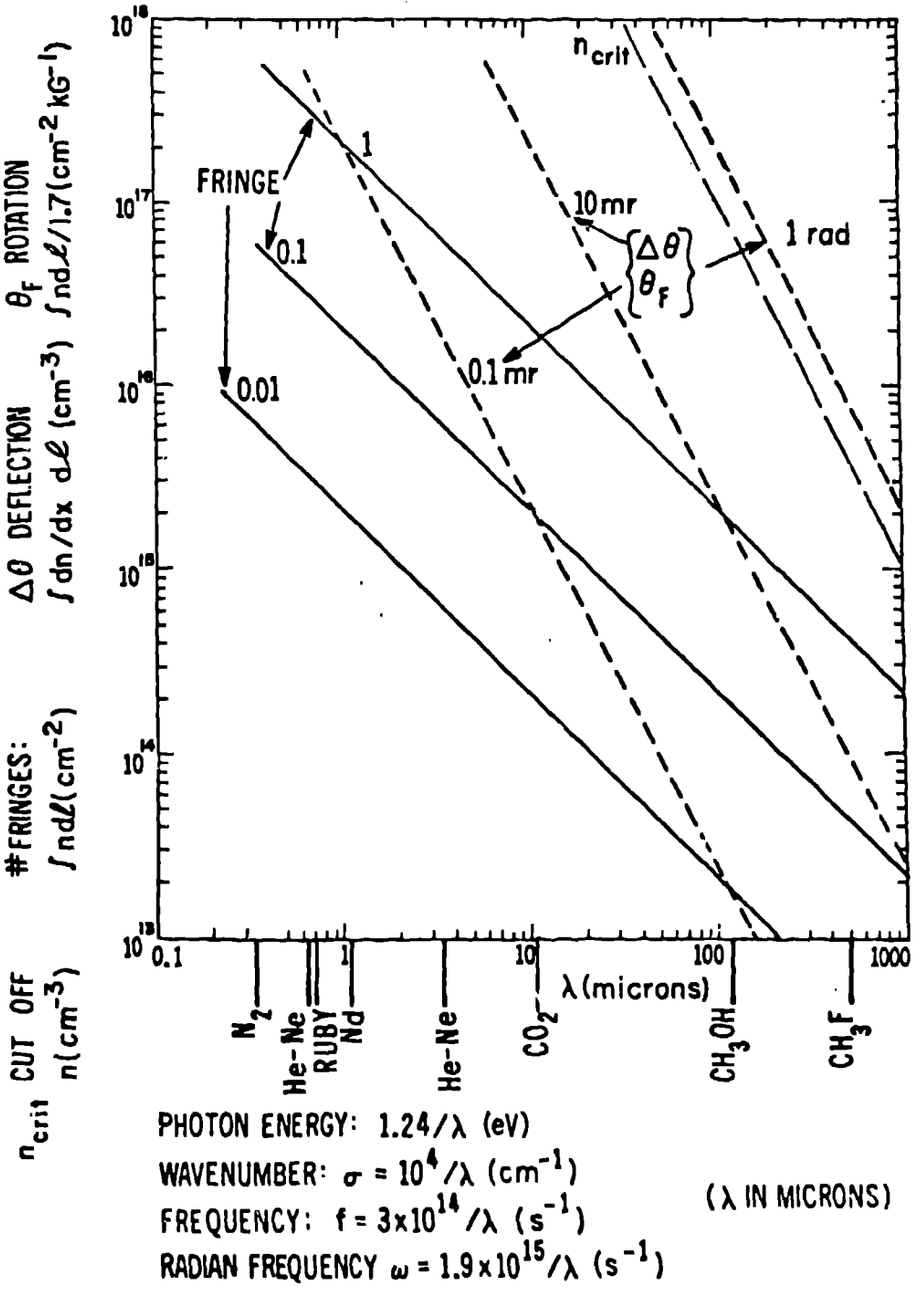

Fig. 1.

Scaling with wavelength of fringe number, Faraday rotation, angular deflection, and critical density.

B. Interferometry

Interferometry is conceptually the most direct technique for measurements exploiting plasma refractivity. It leads directly to an integrated line-of-sight density determination by comparing the optical path length through a plasma with the equivalent optical path length in the absence of plasma. It is "self-calibrating" in the sense that the observed fringe displacement, $f = \int_0^{\ell} (\mu-1)/\lambda \; d\ell$, for a given wavelength is directly related to $\int_0^{\ell} n_e \; d\ell$ through 11.1.16 of I. or Fig. 1.

The following text is divided into A) spatial coverage (line-of-sight integrated, pending unfolding) at one instant in time and B) temporal coverage integrated along one line of sight. Both have good space and time resolution in the sense defined in the introduction.

1. Holographic Interferometry

The introduction in the early 60's of pulsed lasers significantly eased the making of plasma interferograms by providing a light source bright enough to compete favorably with plasma luminosity, and of sufficient monochromaticity and low divergence to relax the severe constraints of path length equality in scene and reference beams (see I.). The introduction of holographic interferometry completed the conversion of an exacting art requiring restrictive specialized instruments to a rather simple procedure that can be improvised in numerous, flexible embodiments.

(The discussion of holographic interferometry at the end of I. is supplemented by the second hand-out,[2] and referenced hereafter as II. A LA-MS report[3] dwells more on practical implementation details, as well as an interesting case of unfolding the radial density distribution for a case of helically deformed cylindrical symmetry.)

The significant feature of holographic interferometry that is responsible for the great experimental simplification is that, in effect, phase comparison occurs between two wavefronts separated in time rather than in space. Phase distortions in the optical path that remain fixed in time between the separate exposures cancel out rather than having to be matched in spatially separated beam paths.

The price paid for the convenience of holography is in the greater coherence requirement on the laser source and the high resolution required of the recording medium. A recent reference[4] gives a good discussion of high coherence pulsed ruby lasers.

A more recent example of an exact analogue of conventional plasma interferometry made possible only by the flexibility of holographic interferometry is the examination of the blow-off of laser fusion targets on micron-size scale lengths.[5] The incorporation of microscope objectives in the scene path and the need for the very precise focusing that can only be achieved during reconstruction require the holographic implementation. The refractive bending for a wavelength fully 1/4 the critical wavelength is quite severe, but because total path lengths involved are extremely short the fractional fringe error (11.3.9 in I.) which scales with ℓ^2 is completely negligible. Focusing in the proper image plane is critical, however, and a good discussion of residual position errors due to path curvature is given in Ref. 6.

Another example when holographic flexibility can be invoked are cases in which conventional interferograms would be too sensitive, i.e., the fringe count exceeds easy resolution. The two holographic exposures can be timed to both occur during the event and thus record only the difference over a pre-selected time interval. By proper manipulation of polarization optics even the linear background fringe pattern can be retained.[7]

The lowest $\int n_e d\ell$'s measurable with holographic interferometry are larger than the sensitivity limits for the CW laser time coverage interferometry described below. One reason is the lack of good equivalents for photographic recording (as well as fewer suitable laser sources) at wavelengths greater than the visible.

Since the publication of II. the use of thin film bismuth has been realized for plasma interferograms by Kristal[8] at the 3 μm HF laser wavelength, and both bismuth film and cuprous mercuric iodide have been used at the 10.6 μm CO_2 laser wavelength by Forman et al.[9] The disappointingly slow progress of long wavelength, high spatial resolution recording media is probably due to the fact that increase in fringe count at long wavelength is

unique to free electron refractivity and the sensitivity actually decreases for non-plasma related holographic applications.

A second reason for the poorer lower sensitivity limit is that in the conventional analysis of a photographically recorded fringe pattern it is much more difficult to measure small fractional fringe displacements (say anything substantially less than 0.1) than with the electronic means for time variation at single space points that can, with care, do better than 0.001 fringe.

In this connection interesting possibilities, not yet to my knowledge applied to plasmas, are raised by heterodyne holographic interferometry, reviewed by Dändliker,[10] in which the use of two reference beams and controlled phase manipulations with the reconstruction beam leads to accurate electronic detection of extremely small fractions of a fringe. The fact that the holographic exposure and reconstruction generally occur at different wavelengths would complicate the geomtery but not pose insurmountable difficulties.

Another disadvantage of holographic interferometry compared to conventional interferometry shows up when a time sequence of interferograms during a single event is required. It is due to the requirement of accurate registry of two exposures for each interferogram frame--one before and one during the event. Initial attempts of "live-fringe" interferometry, comparison of a sequence of current wavefronts in real time with a holographically recorded previous wavefront, are given in II. The method should be easier now with the availability of tunable dye-lasers giving a wider choice of laser sources. Only the initial holographic exposure requires holographic quality source coherence, and it could be made with a lower energy source over a longer exposure time. The observation source must be tuned to the same wavelength, but has more modest coherence requirements and requires a brightness governed only by the combination of reconstruction efficiency, desired time resolution and recording medium sensitivity. Note the latter may be electronic, and does not require holographic quality spatial resolution.

An intriguing possibility for very fast time resolution of very brief total duration events is offered by the combination of short laser coherence length combined with traversal time of the holographic plate by an obliquely incident reference beam.[11] Application to a (small) plasma would require the

plasma to be located near the divergence point of the scene beam with a geometry analogous to that of Fig. 1 in reference 11.

2. Continuous Time Coverage Interferometry

For continuous time coverage during the evolution of a plasma discharge along a single line of sight by use of a CW gas laser the "coupled cavity" configuration was principally emphasized in I. This use of the laser as both the source and the phase sensitive detector, requiring only a small percentage feed-back into the laser cavity, remains the simplest possible experimental configuration. With a moving return mirror the vernier principle of measuring plasma effects by the time distortion of zero crossings could at that time be read to about 1/20 of a fringe from oscilloscope traces. In the interim computerized automated data acquisition from transient waveform digitizers requiring only about four 6-bit data words per cycle has been shown capable of about 1/600 fringe resolution.[12] The supposition that the method would work equally well at far-infrared wavelengths was borne out at 337 microns.[13] An additional benefit of significance in the far infrared is that the laser wavelength could be determined to 0.6% from only a knowledge of the rotating wheel radius without other means of spatial dispersion. (Note that since the coupled cavity configuration necessarily involves a double pass through the plasma, the factor 2 length gain was incorporated into the proportionality constant in I. This is <u>not</u> the convention in either Fig. 1 or the present write-up.)

Coupled cavity interferometry also suffers from some disadvantages. Among these are 1) the time response is limited by the Q-value of the laser cavity, 2) the mechanical modulation reference frequency is available for monitoring only prior to rather than during the measured event, and 3) it is difficult to synchronize more than one channel to a given event. In addition, the increasing technological sophistication of the laser industry has made it much more difficult to find He-Ne lasers operating simultaneously at 0.63 and 3.39 microns, thereby obviating the real alignment simplicity when the greater sensitivity and time response of the longer wavelength is desired.

The cited problems of coupled cavity interferometry are largely overcome by returning to some conventional interferometer configuration of scene and reference beams combined on a detector, but retaining a beat frequency on the detector even in the absence of plasma phase shifts by deliberately introducing a frequency off-set between the two beams. In principle this can be done by a mechanical motion Doppler shift in one beam, like the moving return mirror in coupled cavity interferometry. In practise, it is much preferable to use an acoutso-optic Bragg cell.[14] This can easily produce much larger frequency differences between the zero and first order diffracted beams than any mechanical means, while simultaneously acting as the first beam splitter. The Bragg cell drive frequency is always available as a reference frequency against which the plasma phase shifts can be analyzed. Since it is continuously available, there are no synchronization problems.

Note that this beat frequency distortion measurement is commonly referred to as heterodyne interferometry and is entirely different from the usage of the same term in 11.4.1.6 of I. for the much less practical, though more sensitive, procedure of putting the plasma directly inside the laser cavity and monitoring the laser frequency pulling.

If the reference and scene beams are unequal in length, it is extremely important to prevent any retro-reflection from getting back into the laser and causing a coupled-cavity (and frequency pulling) effect. For unequal paths, laser frequency changes are indistinguishable from plasma changes occurring during the transit time difference interval.

When the heterodyne frequency is chosen to be large compared to the frequency with which plasma effects are to be resolved further analog signal processing before digitization for computer processing can be very useful. For instance, Jacobson[15] describes a five-channel quadrature interferometer in which the plasma phase shift within a chosen bandwidth is determined with unambiguous sign by first mixing the heterodyne detected signal both with the Bragg cell reference frequency and the same reference frequency phase shifted 90° to give analog signals proportional to the sine and cosine, respectively, of the plasma phase shift. A more detailed description on a seven-channel version of this instrument, illustrative also of what can be learned about density fluctuations by correlations among the channels will be published shortly.[16]

C. Faraday Rotation

The discussion of experimental measurements of Faraday rotation in I. emphasizes maximizing sensitivity by increasing the accuracy with which small polarization rotation angles can be measured. An extension of this approach to the 10.6 μm wavelength of the CO_2 laser with a good discussion of the optimum angular orientation of the analyzer has been given by Jarboe.[17]

A different approach is to increase the laser wavelength to take advantage of the λ^2 scaling while simultaneously negating the deleterious effect of the beam bending which has the same scaling, and was assumed to be a fundamental limitation in I. A basic principle in this case is to make the measurement independent of laser intensity variations, as could happen, for instance, due to beam wandering over the detector.

One way to do this is to convert from an amplitude measurement to a phase measurement, in which the signal can be treated exactly as in a heterodyne interferometry set-up. The idea is to produce a sinusoidal modulation in the absence of plasma on which the Faraday rotation is encoded as a time-varying phase shift.[18] A way to do this is to monitor a rotating linear polarization behind a linear polarization analyzer. The rotating linear polarization is the equivalent of, in fact, it is generated by, two frequency off-set (coherent) counter-rotating circular polarizations. The plasma birefringence in a longitudinal field increases the phase velocity of one circular polarization and slows down the phase velocity of the other, resulting in a distortion of the apparent rate of rotation of the linear polarization. In a current Los Alamos version of this experiment[19] a 1 MHz frequency offset is produced between two parts of a 185 μm CO_2-pumped CH_2F_2 laser beam by Doppler shifting a portion of the beam by reflection from a grating machined onto the rim of an 18-cm radius aluminum disk rotating at 6000 rpm. The algorithm previously cited[12] can detect 10 mr beam polarization rotations, which at this wavelength corresponds to $\int n_e \cdot \vec{B} d\ell = 1.1 \times 10^{15} cm^{-2}$ kG, with 1 μs time resolution.

An alternative method achieves the same end, insensitivity to laser intensity variations, by rocking the input linear polarization about the orientation of the analyzer on a time scale fast compared to plasma changes. One detector/analyzer combination rather than two then measures the intensity

increase and decrease, respectively, due to plasma induced rotation for positive and negative orientation with respect to the polarization analyzer. In the far-infrared spectral range the polarization modulation has been achieved with a 1 kHz voltage drive of a ferrite slab.[20] The same effect can be achieved without the severe laser attenuation by the ferrite if two frequency offset coherent orthogonal linear polarizations are observed through an analyzer approximately aligned with one of the polarizations. In both cases because one ends up with an intensity measurement of the envelope of a particular modulation frequency, the time resolution will be poorer but the sensitivity can be made greater than the phase measurement method of a rotating linear polarization.

In pushing Faraday rotation measurements into the far infrared it is necessary to re-examine the linear birefringence in a transverse magnetic field component, which was dismissed as a higher order effect in the introductory section. The circular birefringence in a longitudinal field, $\Delta\mu_{\pm} \approx \omega_p^2\omega_{b\parallel}/\omega^3$, leads to 11.3.18 of I:

$$\theta = 2.63 \times 10^{-17}\ \lambda^2 \int n_e\ B_\parallel d\ell$$

The linear birefringence in a transverse field, $\Delta\mu_{\perp} \approx \frac{1}{2}\ \omega_p^2\ \omega_{b\perp}^2/\omega^4$ (see e.g. Ref. 21), leads to an elliptization for arbitrary orientation of linear polarization that will give a maximum "dephasing" angle:

$$\theta_{e\ell} = 1.2 \times 10^{-21}\ \lambda^3 \int n_e\ B_\perp^2\ d\ell$$

In general the Faraday rotation angle dominates, but as λ increases the extra power of B in the dephasing angle can more nearly compensate the smaller coefficient. For instance, for typical Tokamak fields with $B_\perp >> B_\parallel$ for a laser beam along a minor cross-section chord, the angles are comparable at the CH_3F wavelength of 496 μm. Nonetheless, the phase measurement of a rotating linear polarization is relatively insensitive to ellipticity until the dephasing angle approaches 90° and destroys the modulation as the ellipse rotates in front of a stationary linear analyzer.

At the other end of the sensitivity range, large angle rotations of visible light indicate megagauss magnetic fields in laser-produced plasmas.[22] The fact that these fields may be generated by an inverse Faraday effect due to the circular polarization components of the laser[23] leads us beyond the non-perturbative criterion of this course.

D. Schlieren and Shadowgraph Methods

Only a few points are added here to the discussion of these methods in I.

a) The statement there that interferometry measures density, whereas schlieren and shadowgraphy measure the first and second spatial derivatives, repectively, is correct but somewhat glib, and therefore perhaps confusing. A phase measurement in terms of fringe displacement in interferometry is relative, and becomes meaningful only in relation to another phase measurement displaced either in space or time. An absolute value determination requires a continuum of measurements between the place (time) of interest and a known null value. An absolute measurement of a deflection angle, on the other hand, is functionally related to an absolute value of density gradient independent of neighboring values either in space or time.

b) Although the sensitivity of interferometry and schlieren are difficult to compare because the latter measures the derivative of the quantity measured by the former, the λ^2 scaling of schlieren compared to the λ scaling of interferometry makes it relatively more significant as longer wavelength lasers come into wider use. However the difficulties of obtaining extended spatial resolution detectors leaves a problem of finding the emergent beam.

c) There is an increasing emphasis on quantitative interpretation based on emergent beam location as opposed to the more qualitative relative intensity measurements emphasized in I. For example, Kellmann[24] gives analytical solutions of deflector angle versus normalized radius for twelve different assumed density profile functions. Recently, Raleigh and Greig[25] have presented a detailed calculation procedure, akin to Abel inversion, for deriving the density gradient profile from a finite set of angular deflection observations.

d) Quantitative deflection mensurements have been made recently, among others, both with the inclined slit method in a largely anionized heated gas channel[25] and with separated Moiré plates on a 0.1 mm diameter totally ionized high density z-pinch.[26]

III. SCATTERINC

A. Free Electrons

1. Outline of theory section Monterey Mini-Course (1978) Lecture Notes[27]

p. 1-5

single electron:

Classical electrodynamics:

Scattered power into 4π: $\int P d\Omega = 6.65\times10^{-25} I$

P (units of power)

I (units of power/cm^2)

For electron velocity $\vec{v}$

Time dependence of instantaneous electron position

frequency shift

(calculation requires retarded time)

Physical argument from "double" Doppler shift

Define $\vec{k} \equiv \vec{k_s} - \vec{k_i}$

no recoil, energy conservation $|\vec{k_s}| = |\vec{k_i}|$

$$|k| = 2|k_i| \sin\theta/2 = \frac{4\pi}{\lambda_i} \sin\theta/2$$

Doppler shift argument gives

frequency shift $\omega = \omega_s - \omega_i = \vec{k}\cdot\vec{v}$

$(\Delta\omega)$

This "foreshadows" result that a collection of independent scatterers for

fixed $\vec{k}(k_1,\theta)$ gives spectral distribution that maps out $f(\vec{v})$

p. 6,7
Many scatterers

$\vec{E}_s$ fields add $\qquad I_s \sim (\sum \vec{E}_s)^2$

either cross-product terms sum to 0 on average (phases uncorrelated)
or cross-product terms do not sum to 0 on average (phases correlated)

For a thermal plasma, the Debye length, $\lambda_D \propto (\frac{T}{n})^{1/2}$, is the scale over which correlations (potential energy) win out over random thermal motions (kinetic energy)

The phase factors $(\vec{k}\cdot\vec{r})$ for the <u>many</u> scatterers within a Debye sphere are all nearly alike (correlated) or range over all values 0 to 2π (uncorrelated) depending on the magnitude of $\vec{k}$:

If $k\lambda_D < 1$	correlated	$\alpha > 1$
$k\lambda_D >> 1$	uncorrelated	$\alpha << 1$

$$\alpha \equiv (k\lambda_D)^{-1} = \frac{\lambda}{4\pi\lambda_D \sin\theta/2}$$

p. 8-16
Formalism of summation procedure:

Involves space-time Fourier transformation of n_e distribution

$$n(\vec{x},t) = c\int\int n(\vec{k},\omega)d^3\vec{k}d\omega$$

superposition of plane waves of wavelength $2\pi/|k|$ and phase velocity $\frac{\omega}{|k|}\cdot\vec{k}$.

$$\frac{d^2P(\theta,\omega)}{d\Omega d\omega} = \frac{I_o}{2\pi} r_o^2 [\hat{h}\times(\hat{h}\times\hat{e})]^2 \lim_{t\to\infty} \frac{\langle |n(\vec{k},\omega)|^2 \rangle}{t}$$

i.e., electrons contribute to extent that required wavelengths of spatial fluctuations and velocity projections occur together.

Can be generally written in terms of classical Thomson cross-section and a "form factor" $S(k,\omega)$

$$\frac{d^2P(\theta,\omega)}{d\Omega d\omega} = N_e I_o \sigma_{Th} S(k,\omega)$$

and specializing for collisionless, unmagnetized, near thermal plasmas

$$S(k,\omega) = \frac{|1+\chi_I|^2}{|1+\chi_e+\chi_I|^2} f_e(v) + Z\frac{|\chi_e|^2}{|1+\chi_e+\chi_I|^2} f_I(v)$$

$$\chi_e = \chi_e\left(\frac{\omega}{kv_e}\right) = -G_e(x)$$

$$\chi_I = \chi_I\left(\frac{\omega}{kv_I}\right) = -G_I(y)$$

$$G_e(x) = -\alpha^2\left\{1-2xe^{-x^2}\int_0^x e^{t^2}\,dt + i\pi^{1/2}xe^{-x^2}\right\}$$

$$G_I(y) = -\alpha^2\frac{2ZT_e}{T_I}\left\{1-2ye^{-y^2}\int_0^y e^{t^2}\,dt + i\pi^{1/2}\,ye^{-y^2}\right\}$$

p. 17

Graphs of spectral function for 3 values of α.

1981 Addenda:

1. The narrow central "ion" feature in the two lower figures on p. 17 assumes $T_e = T_i$ and $Z = 1$.
2. The wavelength scale happens to be drawn for $T_e = 5$ eV, $\theta = 90^o$, $\lambda = 6943$Å. This is an unfortunate specialization. The spectral shape is only a function of α, and a more fundamental abscissa would be in terms of $x = \Delta\omega/kv$ with $\Delta\omega = 2\pi c\Delta\lambda/\lambda^2$.
3. The "electron" feature integrated intensity varies as $1/(1+\alpha^2)$, whereas the total integrated intensity in the limit $\alpha \to \infty$ approaches the $\alpha = 0$ values times $Z/(1+ZT_e/T_i)$.
4. Figure 2 (see next page) plots α as a parameter for given n and T_e, assuming $\lambda = 6943$Å, $\theta = 90^o$, and indicates the scaling for other values of λ and θ. The line for $\alpha = 0.2$ is accentuated as an upper limit for a Gaussian spectrum. If electron temperature is determined from the spectral width assuming a Gaussian shape when α is actually 0.2, an 8% overestimate would result.

p. 18-22

Corrections for a) v/c not << 1
b) B ≠ 0

a) additional force, finite transit time give significant, 1st order v/c effects. The most lucid explanation of the somewhat complicated mathematical derivation known to this author appears in Item 7 of the Bibliography in the Monterey Notes.[28]

b) B changes linear orbits; mathematically interesting complexity -- but small practical significance (see p. 32 of Ref. 27).

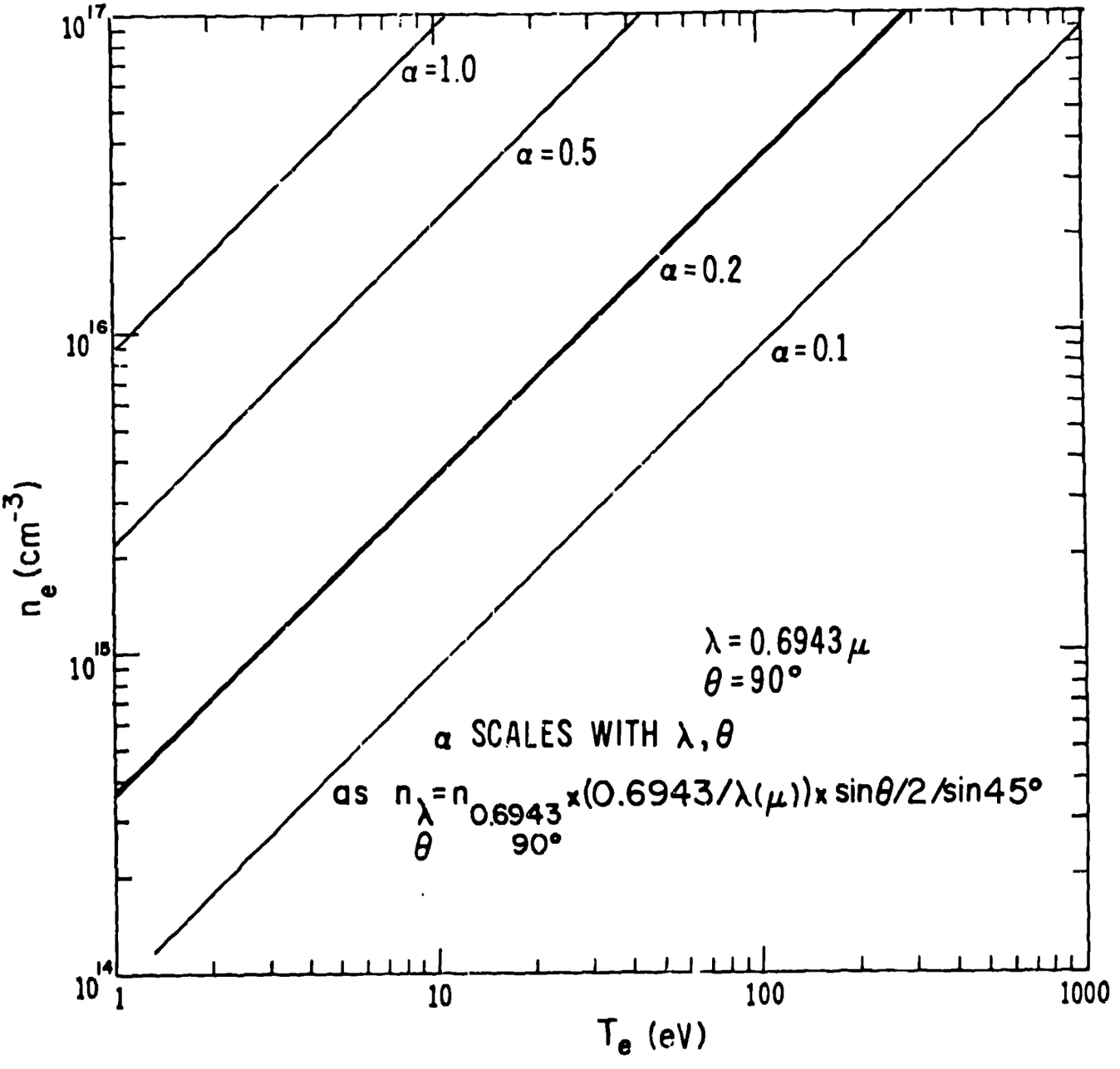

Fig. 2.
Scattering parameter, α, as a function of temperature and density. Scaling with wavelength and scattering angle as indicated.

2. Experimental Considerations, $\alpha << 1$

The practical implementation of a scattering experiment for determination of electron temperature from the Gaussian spectral shape for uncorrelated scatterers ($\alpha << 1$) is dominated by the small value of the Thomson cross-section. The discussion in Ref. 27 from p. 22 onward is relatively straight-forward and not repeated here. It concerns itself with a) availability of powerful sources, b) the number of detected scattered photons, c) signal-to-background or signal-to-background fluctuations ratio, d) stray laser light suppression, e) alignment, f) calibration and g) data acquisition.

A useful discussion of practical aspects encountered in an actual particular experiment is given in Ref. 29.

Absolute calibrations for density determinations have traditionally been done by Rayleigh scattering at the unshifted laser wavelength off a neutral gas, in situ to avoid all scaling for geometrical and detector gain effects. A disadvantage is that either the stray laser light may mask the Rayleigh scattering completely, or a three-stage polychrometer[30] discriminates against the unshifted light so well that the calibration signal doesn't get through. An interesting solution to this problem recently has been the use of anti-Stokes rotational Raman lines in nitrogen[31] and Stokes-shifted Raman lines in hydrogen and deuterium.[32]

The use of avalanche photo-diodes in place of photomultipliers has been reported by DeSilva.[33] One great advantage is a 65% quantum efficiency at 6943Å. It is claimed that their inherent noise is such that the cross-over in S/N ratio compared with photomultipliers favors the diodes above the 10 photons/30 nsec power level. A strong temperature dependence of the photo-diode gain is a definite disadvantage, and the small photo-sensitive area may be another. On the other hand, they open the door to scattering experiments with 30% quantum efficiency at the Nd laser wavelength of 1.06 μm.

The extension of single-space point scattering measurements to simultaneous multiple-space points has become a very active field. Besides the Princeton approach,[34] of which an example is shown in Ref. 27 and which is also being very actively pursued at Los Alamos, a conceptually simple system developed in France[35] based on multiple two-wavelength band spectral ratios is

the basis of the design study of such a system for JET (Joint European Torus). Perhaps to put things into perspective, it is pertinent to mention that the same design study anticipates more than 40 man-years and multi-million dollars to implement this diagnostic.

The extension to multiple-time points, equally important and desirable, is an active research topic, but less advanced. A Garching group[35] has reported 25 equispaced 10 MW ruby laser pulses over a 1 millisecond time period. Work continues at Los Alamos on summing over a mode-locked pulse train. The key problem is an optical switch or a photo-sensitive detector sufficiently fast not to integrate over plasma background between pulses.

3. Comments on $\alpha \geq 1$

The condition α not $<< 1$ means that the combination of incident wavelength and scattering angle is chosen so as to reveal existing phase correlations among the scatterers--i.e., by increasing the wavelength and decreasing the scattering angle to the point that the "probe length" is comparable to the minimum scale length (Debye length) over which correlations can exist.

Choosing these conditions immediately raises a "rich" vein of possibilities--at the very least for a completely quiescent, thermalized plasma there will be correlations among the electron clouds shielding the thermally distributed ions (this is the case for which the form factor given on p. 16 of Ref. 27 applies)--but more likely than not over certain regions in "k" space there will be correlations among the scattering centers (electrons) due to discrete (resonant) plasma waves or plasma turbulence (a spectrum of plasma waves governed by some amplitude distribution in "k" space). By definition these latter correlations are greater than those due to random thermal fluctuations and the received scattered power at the relevant k values may be enhanced by many orders of magnitude.

Notice a change in the focus of interest! To determine electron temperature any one choice of $k > k_D = 2\pi/\lambda_D$ (or for ion temperature any one choice of $k < k_D$) will do, and the thermal distribution is determined by scanning over the scattered wavelength (frequency) spread. To determine a plasma wave or turbulence spectrum we need a scan over k space (generally

obtained over a range of scattering angles) as well as the scan over frequency at each k to determine the total wave strength at that k.

In order to reach the $\alpha \geq 1$ regime for typical magnetic confinement fusion parameters at large scattering angles requires wavelengths in the far infrared. This makes for major differences not only in the source but also in the detector technology.[36]

For example, room temperature detectors operate in the classical regime ($h\nu/kT < 1$) rather than the quantum regime ($h\nu/kT > 1$) and the ultimate noise limitations are quite different. Furthermore, the characteristic frequency shifts of interest, $\Delta\omega \sim \vec{k}\cdot\vec{v}$, are smaller on account of both smaller k values and smaller characteristic velocities (either plasma waves or ion thermal rather than electron thermal velocities) and when the frequency spread of interest is less than the maximum frequency response of the detector it is possible to use heterodyne detection techniques.

Heterodyne detection:

Combine scattered power with coherent local oscillator on a square law detector:

$$E_s = I_s^{1/2} \exp i(\omega + \Delta\omega)t$$

$$E_{\ell o} = I_{\ell o}^{1/2} \exp i\omega t$$

$$I = (E_s + E_{\ell o})(E_s + E_{\ell o})^*$$
$$= I_s + I_{\ell o} + 2(I_s I_{\ell o})^{1/2} \cos\Delta\omega t$$

Response at the beat frequency $\Delta\omega$ can be enhanced by increasing $I_{\ell o}$ alone, and the noise-equivalent-power (NEP) is lower:

$$(NEP)_{het} \sim (NEP)^2_{video}/I_{\ell o}$$

Note also that the local oscillator frequency ω may or may not be equal to the incident laser frequency, ω_ℓ. If $\omega \neq \omega_\ell$, $\Delta\omega$ contains a contribution from this difference as well as from the result of scattering and this moves the

band-pass of the various scattered difference frequencies away from being centered on $\Delta\omega = 0$. This has two advantages:

a. detector noise limitations are generally better away from $\Delta\omega = 0$

b. resolves assymetries in scattered spectrum with respect to the laser frequency.

In turn, heterodyne detection implies a totally different technology for determining the frequency spread (power spectrum). Instead of spectrally dispersing the radiation before detection by separate receivers, one can analyze electronically the frequency components of the signal generated on a single receiver either by filtering or correlation techniques.

The currently favored high-power narrow-band laser for ion temperature measurements is D_2O at 385 μm. An experiment is imminent on Alcator C with a corner-mounted Schottky-whisker diode[37] detector signal Fourier-analyzed into a special design 32 contiguous channel receiver, each channel of 80 MHz width.[38]

The most extensive non-thermal small angle collective scattering on fusion plasmas has been done by Slusher and Surko[39] in a study of density fluctuations. These authors take advantage of the small forward scattering angle for a) coping with the restricted access of diagnostic ports, b) crowding the full range of k values of interest into a smaller range of scattering angles $\Delta\theta$ and c) a convenient geometry for high sensitivity heterodyning--they utilize a 300 watt CW CO_2 laser for the relatively large scattering cross-section of turbulent density fluctuations.

In a companion paper,[40] the small angle geometry disadvantage of lack of spatial resolution is overcome by measuring the correlations of forward scattering from two laser beams intersecting at a shallow angle, with the intersection point moved sequentially through the plasma depth dimension.

Careful consideration must be given at small scattering angles to all the finite geometry effects: diffraction, beam cross-section, finite range of scattering angle, detector size, etc.

B. Light Scattering from Bound Electrons

Consider an electron bound to a nucleus, as opposed to the free electron case treated so far. Classical radiation theory treats such an electron as a damped harmonic oscillator with a natural frequency ω_o corresponding to a particular atomic transition. (Fractional f values then distribute the N such scattering systems among the different possible atomic transitions.) Combination of the equation of motion under the influence of the electric field of the incident light wave, and the radiation from an accelerated charge gives a differential cross-section:

$$\frac{d\sigma}{d\Omega} = \left(\frac{e^2}{mc^2}\right)^2 \sum_i \frac{f_i\ \omega^4}{(\omega_i^2-\omega^2)^2 + \omega^2\Gamma^2}$$

where the damping, Γ, can be calculated self-consistently from energy loss due to scattering to be:

$$\Gamma = \frac{2}{3}\frac{e^2\omega^2}{mc^3} \text{ (cgs units)}$$

Limits: $\omega_i \to 0$ $\qquad \frac{d\sigma}{d\Omega} \to \left(\frac{e^2}{mc^2}\right)^2$ (Thomson differential cross-section)

$\omega \to \omega_i$ $\qquad \sigma \to \lambda^2 \cdot O(1)$

The latter limit can be $\sim 10^{15}$ times the Thomson cross-section, for λ in the visible!

These general features are retained in the correct quantum mechanical calculations, which also add many subtleties.[41]

On resonance the cross-sections are so large that it is sometimes possible to saturate the transition--that is, populate the upper and lower levels in the ratio of their statistical weights. This happens when the number of photon absorptions equals the number of stimulated emissions. An absolute

measurement of the line intensity then yields the ground state population independent of a knowledge of laser intensity or cross-section.

The saturation intensity can be estimated from the requirement that the laser flux be so large that the probability of excitation of any one atom ($\sigma \propto \lambda^2$) over the spontaneous emission lifetime of the excited state ($A^{-1} \propto \lambda^3$) is approximately unity. The resulting intensity has a λ^{-5} dependence. The absolute value is ~100 watts/cm^2-Angstrom at H_α (6563 A), easily obtainable, but 4.6×10^5 watts/cm^2-Angstrom (out of reach!) at Lyman α (1215 A).

A significant further advantage is achieved if there is a radiative transition from the upper level to some other lower level, because the fluorescence can then be monitored on that line without interfering background from the laser radiation.

Diagnostics Applications:

1. Resonant scattering of Lyman alpha (1216 A) as neutral density diagnostic[42]

It is estimated that central neutral densities as low as 2×10^7cm^{-3} should be measurable for PLT or TFTR parameters above the naturally occuring background line radiation originating mainly on the periphery provided the laser source is above 5 KW.

Such sources, based on frequency tripling of 3648 A in a phase-matched gas mixture are just becoming available both at U. of Maryland and in Garching. The 3648 A radiation itself is derived from doubling a laser pumped dye laser.

2. Rayleigh scattering near Hydrogen/Helium lines[43,44]

By staying away from exact resonance one can still maintain relatively large cross-sections, $\sigma \sim 1/\Delta\lambda^2$, while the competing background is the plasma continuum rather than the naturally occurring line radiation itself. This case is generally termed Rayleigh scattering. The scattered intensity spectral breadth for a narrow laser line gives the atomic temperature, and the relative intensity compared to a test gas whose cross-section is also known gives the population density in the lower state for the transition for which

the laser is in near resonance. In the cited references these are n=2 states, and, besides the reduction in sensitivity due to the smaller population resident in these excited states, it requires a plasma model (LTE, coronal, or full rate equations) to relate this number to the total neutral concentration.

3. Neutral impurity studies[45]

Most metallic neutrals have resonance lines in the near UV or at longer wavelengths that can be reached directly or by frequency-doubled dye lasers. In the cited reference a detection sensitivity of 10^6 neutral Fe atoms/cm^3 with a velocity resolution of 0.1 eV has been achieved near the walls of ISX-B with saturation techniques.

4. Miscellaneous

Transport mechanisms can be investigated by generation of impurities[46], or production of metastable levels through optical pumping[47], in a localized region by one laser, and interrogating slightly later at another location with a different laser resonant wavelength.

The time-dependence of the fluorescence response during laser illumination with powers exceeding saturation can be interpreted through the rate equations to give rate coefficients, some of which in turn depend on plasma parameters.[48,49]

At Los Alamos we are currently giving thought to a plasma internal magnetic field direction measurement by observing the timing of a modulated saturated resonance signal generated by absorption of a dye laser. The laser output would be given a rotating linear polarization, it would be tuned to a single Zeeman component, and it would intersect an atomic lithium beam. An even more attractive scheme is to place the plasma inside the cavity of a broad-band dye laser and deduce the Zeeman pattern from intra-cavity absorption caused by the lithium beam.

References

1. F. C. Jahoda and G. A. Sawyer, "Optical Refractivity of Plasmas," in Methods of Experimental Physics Vol. 9B, Griem and Lovberg, eds., (Academic Press, New York, 1971), Chap. 11.
2. F. C. Jahoda, "Pulse Laser Holographic Interferometry," in Gas Dynamic Research, Edited by Dosanjh, (Plenum Press, New York, 1971), pp. 137-154.
3. F. C. Jahoda and R. E. Siemon, "Holographic Interferometry Cookbook," Los Alamos Scientific Laboratory report LA-5058-MS (October 1972).
4. W. Koechner, "Pulsed Holography," in Laser Handbook Vol. 3, M. L. Stich, ed., (North Holland, 1979), Chap. B4.
5. D. T. Attwood, IEEE J. of Quantum Electron. QE-14, 909 (1978).
6. D. W. Sweeney, D. T. Attwood, and G. W. Coleman, Appl. Opt. 15, 1126 (1976).
7. W. T. Armstrong and P. R. Forman, Appl. Opt. 16, 229 (1977).
8. R. Kristal, Appl. Opt. 14, 629 (1975).
9. P. R. Forman, S. Humphries, Jr., and R. W. Peterson, Appl. Phys. Lett. 22, 537 (1973).
10. R. Mindliker, Prog. Opt. 17, 1 (1979).
11. N. Abramson, Opt. Lett. 3, 121 (1978).
12. K. Klare, (Los Alamos National Laboratory-private communication).
13. R. W. Peterson and F. C. Jahoda, Appl. Phys. Lett. 18, 440 (1971).
14. R. Kristal and R. W. Peterson, Rev. Sci. Instrum. 47, 1357 (1976).
15. A. R. Jacobson, Rev. Sci. Instrum. 49, 673 (1978).
16. A. R. Jacobson, submitted to Plasma Physics.
17. T. R. Jarboe, J. Appl. Phys. 48, 557 (1977).
18. G. Dodel and W. Kunz, Infrared Phys. 18, 773 (1978).
19. M. D. Bauman, R. W. Carpenter, and K. A. Klare, (Paper B3O1, this conference).
20. C. H. Ma, D. P. Hutchinson, and K. L. Vander Sluis, Appl. Phys. Lett. 34, 218 (1979).
21. C. B. Wharton and M. A. Heald, Plasma Diagnostics with Microwaves, (John Wiley and Sons, Inc., 1965).

22. J. A. Stamper and B. H. Ripin, Phys. Rev. Lett. 34, 138 (1975).
23. Abraham C. L. Chian, Phys. Fluids 24, 369 (1981).
24. F. Keilmann, Plasma Physics 14, 111 (1972).
25. M. Raleigh and J. R. Greig, NRL Memorandum Report 4390, February 1981.
26. J. E. Hammel, F. C. Jahoda, J. Shlachter, D. A. Platts, Bull. Am. Phys. Soc. 24, 1078 (1979).
27. F. C. Jahoda, "Primer on Laser Scattering Diagnostics," Los Alamos National Laboratory report LA-7400-MS (1978).
28. S. Segre, "Thomson Scattering from a Plasma," in Course on Plasma Diagnostics and Data Acquisition Systems, Varenna 1975, A. Eubank and E. Sindoni, Eds. (Editrice Compositori-Bologna, 1975).
29. J. D. Sethian and C. A. Ekdahl, Rev. Sci. Instru. 49, 729 (1978).
30. R. E. Siemon, Appl. Opt. 13, 697 (1974).
31. J. Howard, B. W. James, and W. I. B. Smith, J. Phys. D: Appl. Phys. 12, 1435 (1979).
32. G. D. Bogomolov and A. A. Letunov, Sov. J. Plasma Phys. 5, 744 (1979). English translation of Fiz. Plazmy 5, 1380 (1979).
33. A. W. DeSilva, Rev. Sci. Instrum. 50, 1605 (1979).
34. J. Lasalle and P. Platz, Appl. Opt. 18, 4124 (1979).
35. R. Behn, H. Röhr, K.-H. Steuer, and D. Meisel, Appl. Phys. Lett. 36, 363 (1980).
36. N. C. Luhmann, Jr., Chapter 1 in Infrared and Millimeter Waves, Vol. 2, Kenneth J. Button, Ed. (Academic Press, 1979).
37. H. R. Fetterman, P. E. Tannenwald, B. J. Clifton, and C. D. Parker, Appl. Phys. Lett. 33, 151 (1978).
38. P. Woskoboinikow, H. C. Praddaude, W. J. Mulligan, D. R. Cohn, Proceedings of the June 1981 CLEO Conference, to be published in IEEE J. of Quantum Electron.
39. R. E. Slusher and C. M. Surko, Phys. Fluids 23, 472 (1980).
40. C. M. Surko and R. E. Slusher, Phys. Fluids 23, 2425 (1980).
41. R. Loudon, The Quantum Theory of Light, (Clarendon Press, 1973). (A good phyical interpretation is given in Rousseau et al., Phys. Rev. Lett. 34, 1306 (1975), while Doppler effects are added by Wrobel, Garching Internal Report IPP 1/160 (1976)).

42. D. W. Koopman, T. J. McIlrath, and V. P. Myerscough, J. Quant. Spectrosc. Radiat. Transfer 19, 555 (1978).

43. H. F. Döbele and K. Hirsch, Phys. Lett. 54A, 267 (1975).

44. W. G. Wrobel, K.-H. Steuer, and H. Röhr, Phys. Rev. Lett. 37, 1218 (1976).

45. B. Schweer, D. Rusbüldt, E. Hintz, H. B. Roberts, and W. R. Husinsky, 4th Int. Conf. on Plasma Surface Interactions, Garmisch-Partenkirchen, April 1980, to be published in J. Nuc. Mat.

46. H. C. Meng and H. J. Kunze, Phys. Fluids 22, 1082 (1979).

47. D. Dimock, E. Hinnov, and L. C. Johnson, Phys. Fluids 12, 1730 (1969).

48. R. M. Measures, J. Appl. Phys. 39, 5232 (1968).

49. D. D. Burgess and C. H. Skinner, J. Phys. B: Atom. Molec. Phys. 7, L297 (1974).